Anose et al. Environmental Systems Research (2022) 11:3
https://doi.org/10.1186/s40068-022-00246-8

Environmental Systems Research

RESEARCH Open Access

Spatiotemporal analysis of droughts characteristics and drivers in the Omo-Gibe River basin, Ethiopia

Fikru Abiko Anose[1*], Kassahun Ture Beketie[1], Tadesse Terefe Zeleke[2], Desalegn Yayeh Ayal[3], Gudina Legese Feyisa[1] and Bereket Tesfaye Haile[1]

Abstract

Background: Drought is one of the leading destructive natural disasters adversely affecting natural resources and livelihoods. Thus, this study evaluated the spatial and temporal meteorological drought characteristics and their drivers in the Omo-Gibe River basin (OGRB) from 1981 to 2017. The drought analysis used the standardized Precipitation Index (SPI) and the Standardized Precipitation Evapotranspiration Index (SPEI) with 4- and 12-month timescales. The Mann–Kendall (MK), Sen's slope estimator, and Pettit test were used to evaluate the trend and change points of the time series. Pearson correlation was used to examine the teleconnection between large-scale global climate signals with the basin's seasonal and annual drought indices.

Results: Accordingly, extreme and severe drought events were observed in 1988, 2000, and 2009. In the basin, prolonged drought events were recorded from 2000 to 2015. The statistically significant ($P < 0.05$) increasing trend of seasonal and annual drought events was observed in all basin parts. However, more drought events distribution was exhibited in the south than in the north and central parts. The Sawla station (southern part) showed a higher drought frequency, ranging from 18.18 to 20.36%. The maximum intensity and peak drought events were observed in this sub-basin, with SPEI reaching − 2.27 and − 4.89, respectively. The global indices NINO3.4, SOI, and DMI are drivers for triggering the meteorological droughts in OGRB.

Conclusions: Substantial warming and erratic rainfall have made OGRB vulnerable to drought events. The intensification of droughts in the basin has also been recorded in humid parts of the basin which has a significant adverse effect on the water availability of down streams. This indicates that the observed drought intensity can increase the water deficit and other natural resources degradation. Therefore, this study provides essential information on drought characteristics for decision-makers to plan appropriate strategies for early warning systems to adapt and mitigate drought hazards in the basin.

Keywords: Drought characteristics, Mann–Kendall trend test, SPI, SPEI, Global indices

Introduction

Drought significantly affects water resources, agriculture, and socioeconomic sectors (Asong et al. 2018; Ghosh 2019; Spinoni et al. 2014; Wang et al. 2014). Unlike other natural hazards such as floods, tornadoes, and hurricanes, drought develops slowly in its onset and impacts; therefore, its effects are felt gradually (Khadr 2016; Kundzewicz and DÖLL 2009; Van Loon 2015). Drought

*Correspondence: fikreabiko@gmail.com
[1] Center for Environmental Science, College of Natural and Computational Sciences, Addis Ababa University, P. O. Box 1176, Addis Ababa, Ethiopia
Full list of author information is available at the end of the article

has no universal definition but can be grouped into four categories such as meteorological, agricultural, hydrological, and socioeconomic drought (Van Loon 2015; Sharafati et al. 2020). Meteorological drought usually precedes agricultural, hydrological, and socioeconomic drought events (Andreadis et al. 2005). The cumulative effect of all types of drought undermines remarkably the ecosystem capacity to provide natural services, e.g., water for hydroelectric power, agriculture, industries, and domestic purposes. Therefore, properly documented drought characteristics are crucial for planning efficient use of water resources, food security, agricultural production, and hydroelectric power (Fenta et al., 2017).

The recent studies highlighted several drought events in Ethiopia from 1980 to 2004 (e.g., Williams et al. 2012; Spinoni et al. 2014; Gebrechorkos et al. 2019) and are expected to continue in the future (Lautze et al. 2003; Gebrehiwot et al. 2011). The famine of 1983–1985 killed one million people, and the current multi-year drought in Ethiopia also proves to be even more disastrous (Richman et al. 2016). Mainly, the drought that occurred in 2002 affected the highest number of people (Viste et al. 2013). Jury and Funk (2013), Degefu et al. (2017), Zeleke et al. (2017) also attested that since 1997 the frequency and severity of drought have increased in southern and southwestern Ethiopia. These recurrent droughts in Ethiopia have disastrous effects on the country's different socioeconomic systems (Teshome and Zhang 2019). Generally, Ethiopia is leveled as the most drought-affected country in Africa. However, most of the earlier studies focused at the country scale. Generalized results covering the whole country would be complex because of the sharp local differences in microclimates (Changnon 2000). Therefore, the detailed finer spatial scale drought examinations are critical to understanding the drought impacts and the regions' varying vulnerabilities. It is used comprehensively to plan and manage drought and associated risks at the regional scale.

The Omo-Gibe River Basin (OGRB) is the second-largest basin in Ethiopia and a very significant resource within the country. The basin has massive irrigation and hydropower dams vulnerable to climate change impacts. In addition, drought events that frequently occurred in OGRB made substantial losses in life and different productive sectors; however, Degefu and Bewket (2015) did only a single study in the basin. This aforementioned study used a small number of stations to represent the entire basin and indices based on precipitation only. Notably, it did not include the stations found in the humid (central) part of OGRB. Moreover, most of the climate-related studies in Ethiopia focused only on the northern and central parts of the country. This information indicates that no comprehensive study encompassing drought characteristics in the basin scale has been done. Thus, to fill these gaps, the current study used different methods to evaluate drought incidences in OGRB. To this end, two metrological drought indices; the Standard Precipitation Index (SPI) (McKee et al. 1993) and the Standardized Precipitation and Evapotranspiration Index (SPEI) (Vicente-Serrano et al. 2010), were used.

The climate of Ethiopia is mainly influenced by the seasonal migration of the Inter-Tropical Converging Zone (ITCZ), the complex topography, and the teleconnection of global atmospheric circulation (Endris et al. 2016; Workie and Debella 2018). For instance, the El Niño-southern oscillation (ENSO) was the ultimate cause of the most drought years in Ethiopia, particularly in 2015 (Funk 2012). Although several studies were done on the influence of global climate change on Ethiopian frequent drought incidences [e.g., Funk 2012; Degefu et al. 2017; Zeleke et al. 2017; Dubache et al. 2019)], however, there is still an absence of evidence about the basin. Based on this fact, this study examined the link between seasonal and annual drought occurrence and selected global climate indices.

Hence, the objectives of the current study are to (i) evaluate the spatiotemporal variation of drought characteristics (frequency, severity, and intensity) in OGRB from 1981 to 2017, (ii) the seasonal and annual trend of drought occurrence using SPI/SPEI with 04 and 12-month time scales, and (iii) the teleconnection between the global driving forces with seasonal and annual drought indices. This study is the first of its kind for this particular basin to identify drought characteristics using the SPI and the SPEI for 4-months and 12-months of timescales in the basin. The results would be helpful for drought risk management and sustainable watershed management and decision-making in the basin. Furthermore, the location and biophysical features of the basin represent the majority of Ethiopia's agroecology, and hence, the result could be applied to other parts of the country.

Methodology

Study area

There are twelve river basins in Ethiopia. Omo-Gibe River basin is an essential basin of southwest Ethiopia and lies between 4°30′ N to 9°30′ N latitude and 34°44′ E to 38° 24′ E longitude. It is the second-largest river basin after Abbay in Ethiopia (Fig. 1), having on average 79,000 km^2 size, 550 km length, and a breadth of 140 km. It has an annual discharge of 16.6 BMC (Billion Cubic Meters), accounting for 14% of Ethiopia's annual surface water resource. The northern and central half of the basin lies at an altitude greater than 1500 m.a.s.l. with a maximum elevation of 3360 m.a.s.l. (located between Gilgel-Gibe

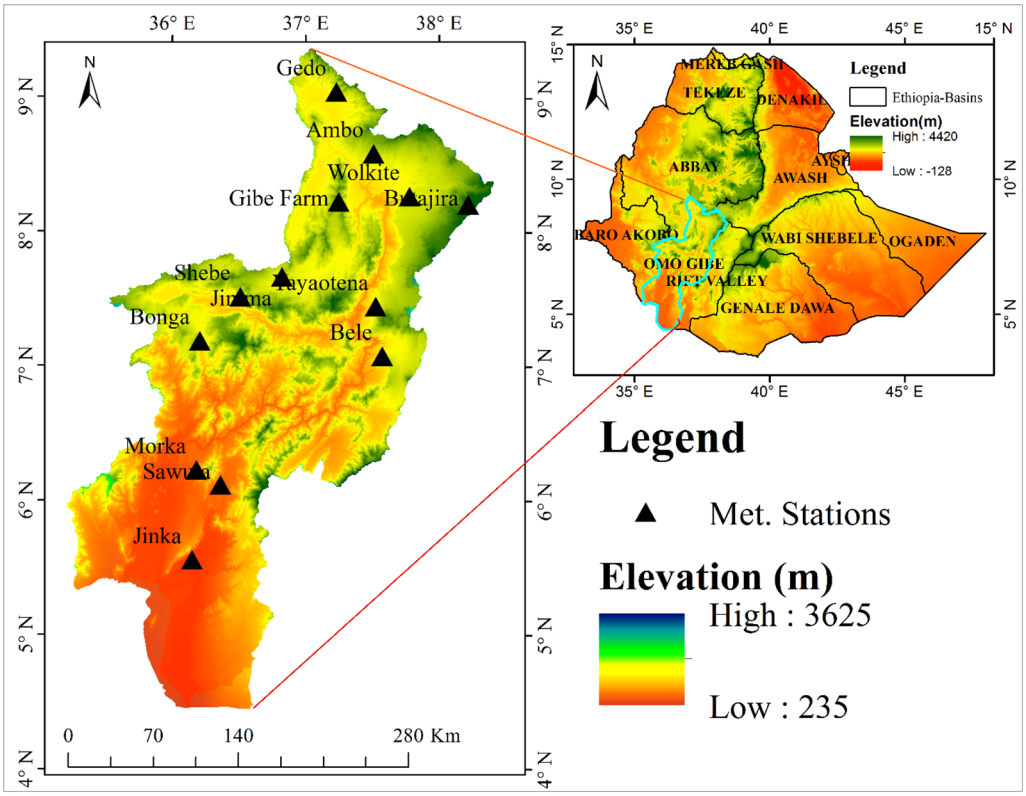

Fig. 1 Topographic map and spatial distribution of the meteorological stations in the OGRB

and Gojeb tributaries).Moreover, the plains of the lower basin lie between 200 and 500 m.a.s.l (Shiferaw et al. 2018). It runs from the northern highlands through the lowlands and into Lake Turkana near the Ethiopian-Kenyan border in the south. It is supplied along the way by several significant tributaries (Avery 2010). The Ethiopian government has been planning massive hydroelectric and irrigation projects. In general, five cascaded dams for hydroelectric power plants are planned for the basin, with a total capacity of 4914 MW. Among these, Gibe I, II, and III dams are operational, while Gibe IV and V dams are planned for future power generation (EEPC 2010). In the OGRB, there are substantial irrigation projects.

Ethiopia has three climatological rainy seasons, namely, the Kiremt season (June to September), the Bega season (October to January), and the Belg season (February to May) (Viste et al. 2013; Temam et al. 2019). Except in the basin's southern part, the central and northern parts receive a monomodal rainfall pattern. The southern part has a bimodal pattern of rainfall, which depends on rainfall in the *Belg* season (February to May) and receives a short period of rainfall in the Bega season from October to January (Degefu 1987; Gissila et al. 2004). Annual rainfall in the basin varies from 400 mm in the extreme south low land to more than 2000 mm in the highland area. The mean annual temperature in the basin varies from less than 17 °C in the West highlands and more than 30 °C in the southern lowlands. The basin's climate is characterized by an arid and semiarid climate in the southern part and a tropical humid one in the northern and the central parts of the basin (Gebre Michael et al., 2005). The mean annual rainfall minimum and maximum temperature of the basin are shown in Fig. 2.

Data processing and quality control

The most fundamental barrier that hinders regional studies such as drought monitoring is the long-term recording and quality of climatic data. The high-resolution gridded data is critical for a region like Ethiopia, where stations are rare and dispersed. Therefore, high resolution (i.e., 4 × 4 km) combined satellite and station data were used to remove missing data and record time differences in observed data from stations. This dataset fills spatial and temporal gaps in Ethiopia's national observations data. It merges quality-controlled station data from the national observation network with locally calibrated satellite-derived data (Dinku et al. 2014). The monthly rainfall and minimum and maximum temperature data

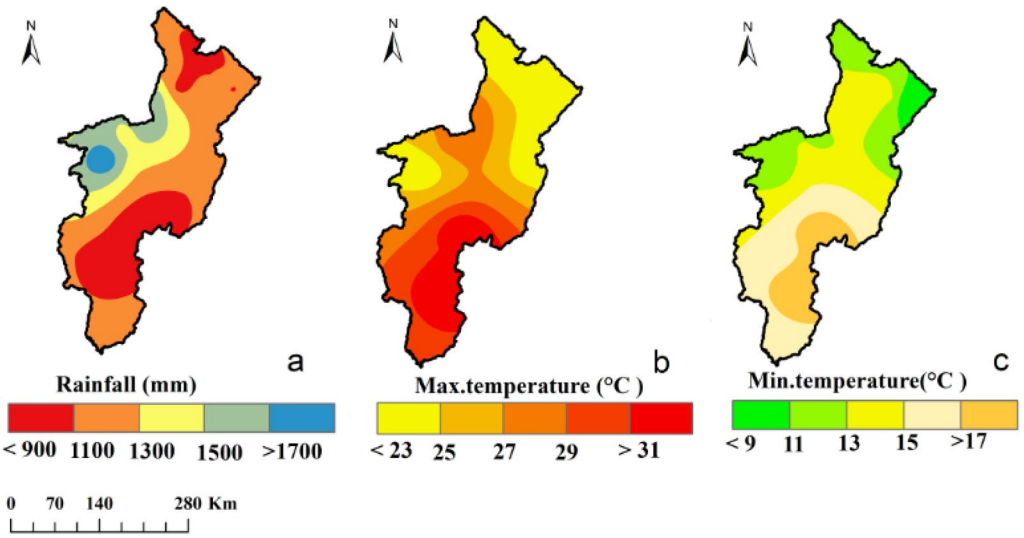

Fig. 2 The spatial distribution of the mean **a** annual rainfall, **b** annual maximum temperature, and **c** annual minimum temperature in OGRB from 1981 to 2017

Table 1 Meteorological stations of OGRB according to the three sub-regions

Sub-basin	St_Name	Latitude (°)	Longitude (°)	Elevation (m)
Northern	Ambo	8.59	37.51	2560
	Butajira	8.21	38.22	2210
	Gedo	9.05	37.23	2500
	Gibe Farm	8.23	37.25	1510
	Wolkite	8.27	37.78	1884
Central	Bele	7.08	37.58	1240
	Bonga	7.19	36.22	1661
	Jimma	7.67	36.83	1725
	Shebe	7.52	36.52	1655
	Yayaotena	7.45	37.53	1537
Southern	Jinka	5.56	36.17	1373
	Morka	6.23	36.2	1221
	Sawula	6.12	36.38	1347

from 1981 to 2016 were obtained from the Ethiopian National Meteorological Agency (NMA) (http://www.ethiomet.gov.et/). Before being disseminated, the data quality was checked and recognized through a collaboration between Enhancing National Climate Service (ENACTS) and NMA (Dinku et al. 2018). Hence, this intensive and free of missing data were used to compute drought distribution and characteristics in the basin. The rainfall and temperature data were checked for autocorrelation before a trend test. Finally, thirteen stations were selected and grouped into three sub-basins: northern, central, and southern parts (Table 1).

The study also applied the leading global climate indices (Niño3.4, SOI, and DMI) that influence Ethiopia's drought variability and frequency. These global climate indices were the SST anomaly index (NINO 3.4), Southern Oscillation Index (SOI), which measures the difference between the Tahiti and Darwin sea level pressure anomaly, and the Indian Ocean Dipole indices referred to as Dipole mode index (DMI) (Saji et al. 1999). They were obtained from (http://www.esrl.noaa.gov/psd/gcos_wgsp/Timeseries/Data/nino34, https://psl.noaa.gov/gcos_wgsp/Timeseries/SOI/, and http://www.jamstec.go.jp/frcgc/research/d1/iod/DATA/dmi).

Drought indices

Different meteorological indices have been used to analyze drought characteristics in different areas (Morid et al. 2006), including the standard precipitation index (SPI) (McKee et al. 1993), the Palmer drought severity index (PDSI) (Palmer 1965), and the standardized precipitation and evapotranspiration index (SPEI) (Vicente-Serrano et al. 2010). Like SPI, SPEI is multiscalar, and besides precipitation, it includes temperature data to evaluate the potential evapotranspiration (PET) and to calculate climate water balance (CWB) (Hänsel et al. 2019). Moreover, the SPEI also combines the sensitivity of PDSI to changes in evaporation demand with the simplicity of calculation and the multi-temporal nature of the SPI (Vicente-Serrano et al. 2010). The SPI and SPEI are useful to assess drought events in arid-dominated regions such as East Africa (Ntale and Gan 2003). In addition, using different drought indices provides a complete picture of the spatiotemporal distribution

of the drought in the basin (Temam et al. 2019; Alsafadi et al. 2020).

Standardized precipitation index

The SPI evaluates drought in precipitation deficit impacting groundwater availability, soil moisture streamflow, and reservoir storage (WMO 2012).To calculate the SPI, a long-term precipitation record is needed. First, an appropriate probability density distribution is fitted to the frequency distribution of cumulated precipitation, and then it has been subsequently converted to a standard normal distribution. The gamma distribution (two parametric), which generally fits better to precipitation data, is used (Wang et al. 2014; Irannezhad et al. 2015). A detailed description of the complete computations of the SPI is found in the paper of (Zeleke et al. 2017).

Standardized precipitation evapotranspiration index

The SPEI is one of the most widely used drought indices to understand meteorological, agricultural, and hydrological drought impacts around the globe (Wang et al. 2014; Labudová et al. 2017; Yang et al. 2019). It is selected as a robust one for regional drought monitoring and analysis considering global climate change scenarios because of its ability to identify the effects of temperature on drought conditions (Liu et al. 2016). The SPEI is mainly selected to evaluate the role of temperature through its influence on potential evaporation, which relates to global warming and the occurrence of drought (Meza 2013; Manatsa et al. 2017). The SPEI is computed using precipitation (P) and PET as input variables resulting in the climate water balance (P-PET) outputs (Vicente-Serrano et al. 2010). Including the widely used Penman–Monteith (PM) method, several methods have been introduced to calculate (PET) (Allen et al. 1998). However, the PM method requires full meteorological data, which is challenging to get in many parts of the world. Thus, the PET can be estimated using Hargraves (Hargreaves and Samani 1985) method, which has a similar output as PM (Beguería et al. 2014). Hargraves method needs only precipitation, minimum, maximum temperature and is the extraterrestrial radiation (R_a) (Senay et al. 2011). Hence, in this study, the Hargraves method was used to calculate the PET.

$$PET_{HG} = 0.0023 \times (T_{mean} + 17.8) \times \left(\sqrt{T_{max} - T_{min}}\right) \times Ra \quad (1)$$

where: PET_{HG} is potential evapotranspiration of Hargreaves method (mm/day),R_a is the extraterrestrial radiation (mm/day), calculated theoretically as a function of latitude, T_{mean} is the average temperature (°C), T_{max} and T_{min} are the maximum and minimum temperature (°C), respectively. Once PET was estimated, D_i calculated using the difference between precipitation and PET as in Eq. (2)

$$D_i = P_i - PET_i \quad (2)$$

where: D_i is climatic water balance (CWB) in a given period (mm), P_i is monthly precipitation in a given period (mm), PET_i is the monthly potential evapotranspiration (mm). The accumulated difference between P and PET in different time scales can be calculated as

$$D_n^k == \sum_{i-0}^{k-1} (P_{n-i} - PET_{n-i}) \quad (3)$$

where: k is a different time scale, and n is the number of calculations. The function of log-logistic distributions gives better results than other distributions for obtaining SPEI series in standardized D with a mean of zero and standard deviation of one (Vicente-Serrano et al. 2010; Potop and Možný 2011).

$$f(x) = \frac{\beta}{\alpha}\left(\frac{x-\gamma}{\alpha}\right)^{\beta-1}\left[1 + \left(\frac{x-\gamma}{\alpha}\right)^{\beta}\right]^{-2} \quad (4)$$

where: α, β, and γ are scale, shape, and location parameters, respectively, for D values in the range ($\gamma < D < \infty$). Therefore, the probability distribution function can be expressed as follows

$$F(x) = \frac{\beta}{\alpha}\left[1 - \left(\frac{\alpha}{x-\gamma}\right)^{\beta}\right]^{-1} \quad (5)$$

The SPIE can easily be obtained as the standardized $F(x)$ with an approximation of

$$PEI = W_i - \frac{2.515517 + 0.8022853\mathrm{W_i} + 0.010328\mathrm{W_i}^2}{1 - 1.432788\mathrm{W_i} + 0.189269W_i^2 + 0.001308\mathrm{W_i}^3} \quad (6)$$

while for $p \leq 0.5$, $W_i = \sqrt{-2\ln(p)}$, whereas if $p > 0.5$, $W_i = \sqrt{-2\ln(p)}$ where: p is the probability of exceeding a determined D value, p=1-F (x). If p>0.5, then p is replaced by 1-p and the sign of the resultant SPEI is reversed (Table 2).

Evaluating drought characteristics

Drought characteristics can be evaluated by the following essential features: duration, frequency, intensity, severity, and spatial and temporal extent (Alamgir et al. 2015; Fanta and Disse 2018). In this study, the drought occurrence evaluated only months with SPI/SPEI ≤ −1 (moderate, severe, and extremes), because the mild drought values slightly vary from the normal one. The duration, severity, intensity, and frequency of the drought events are calculated based on (Table 2).

Table 2 Classification of the severity of drought events on the calculation of SPI/SPIE (McKee et al. 1993)

Categories	SPI/SPIE values
Extremely dry	≤ -2.0
Severely dry	-1.5 to -1.99
Moderately dry	-1.0 to -1.49
Near normal	0.99 to -0.99
Moderately wet	1.0 to 1.49
Severely wet	1.5 to1.99
Extremely wet	≥ 2.0

I. The frequency is the number of months that the SPI/SPEI value meets a set value (Table 2) divided by the number of months in the entire series (Wang et al. 2014).

$$F = \frac{n}{N} \times 100 \tag{7}$$

where: n is the number of months drought events (SPI/SPIE ≤ -1) that an index value meets a set drought criterion divided by the number of months in the entire series (N). Drought frequency (F) was used to assess the drought prevalence during the study period.

II. Duration is the length of a drought episode. Magnitude (M) is the cumulative sum of the index value based on the duration of drought occurrence

$$M = \sum_{i=1}^{Duration} Index \tag{8}$$

III. The intensity (I) of a drought event is the magnitude divided by the duration. Events that have a shorter duration and higher severity will have larger intensities.

$$\mathrm{I} = \frac{\text{Magnitude}}{\text{Duration}} \tag{9}$$

The 4-months seasonal division is best to represent the seasonal precipitation patterns in the area. Hence, in this study, the 4-month accumulation of SPI/SPEI is to evaluate the seasonal or which is essential to know agricultural drought events, and the 12-months accumulation of SPI/SPEI is used to assess the annual or which is used fully to analyze the hydrological drought events (Giuseppe et al. 2019; Alsafadi et al. 2020). To compute SPI and SPEI indices the SPEI package in R statistical program was used. The package was developed by (Beguería et al. 2010) and is freely available at http://digital.csic.es/handle/10261/10002.In this website, detailed information on the computational algorithm is found (Manatsa et al. 2017). In addition, the inverse distance weighting (IDW) method was used to visualize the spatial patterns of the drought events in the basin.

Trend analysis of drought

In the current study, the drought trend has been done using the non-parametric Mann–Kendall test (MK) (Mann 1945; Kendall 1975). The MK test is used to evaluate a statistical significance (increasing and decreasing trend) for meteorological variables, the seasonal and annual trend of SPI/SPEI–4, and 12-months timescales. The MK is a non-parametric statistical method that is robust and suitable for detecting trends since it is less sensitive to outliers within time series data. The MK statistic (S) is mathematically computed as follows:

$$S = \sum_{i=1}^{N-1} \sum_{j=i+1}^{N} sgn(x_j - x_i) \tag{10}$$

$$Z_s = \begin{cases} \frac{S-1}{\sqrt{Var(S)}}, S > 0 \\ 0, S = 0 \\ \frac{S+1}{\sqrt{Var(S)}}, S < 0 \end{cases} \tag{11}$$

where: Z_s is the standard test statistics. The statistical significance level of the trend variation was evaluated using Z_s value. A positive value of Z_s indicates an upward trend, while a negative value of Z_s indicates a downward trend. The value $|Zs| > 1.96$ indicates a significant upward/downward trend. The result of the MK test has been affected by the autocorrelation of the time series (Yue and Wang 2002; Tian and Quiring 2019). Therefore, before the MK trend test was applied on the time series, the autocorrelation tests had been done to see the natural trend in the data (Alexander et al. 2009).

Sen's slope estimator

Sen's (1968) slop estimator has been widely used to detect the trend direction and determine the magnitude of the time-series change. Sen's slop is the non-parametric method to calculate the change per unit time (Pal et al. 2017). Moreover, the MK test can be complemented with Sen's slope estimator. The negative slope value indicates the increase of drought, whereas the positive slope indicates the increase of wetness.

Tests for change-point detection

The Pettitt test is a non-parametric test that has been used in several climate studies to detect abrupt changes in the mean distribution of the variable of interest. The test statistic $U_{t,T}$ is assessed for all random variables from 1 to T; then the most significant change point is selected

where the value of $\left|U_{t,T}\right|$ is the largest (Jaiswal et al. 2015). To identify a change point, a statistical index U_t is defined as follows:

$$U_{t,T} = \sum_{i=1}^{t}\sum_{j=1}^{T} Sgn(x_i - x_j), \quad 1 \le t \le T \tag{12}$$

where similar to the MK test,

$$Sgn(\theta) = \begin{cases} +1 & \theta > 0 \\ 0 & \theta = 0 \\ -1 & \theta < 0 \end{cases} \tag{13}$$

The most probable change point is found where its value is (The break occurs in year k when). The test statistic K_n and the associated probability (P) used in the test are given as.

$$K_{t_0} = \max_{1 \le y \le n} \left|U_{t,T}\right| \tag{14}$$

and the significance probability associated with value K_t is evaluated as

$$p_{(t_0)} = 2exp\left[\frac{-6k_{t_o}^2}{T^3 + T^2}\right] \tag{15}$$

where: t_0 is concluded as a significant change point when $P_{t_0} \le 0.5$. The value is then compared with the critical value given by (Pettitt 1979). Given a certain significance levelα, if $p < \alpha$, we reject the null hypothesis and conclude that x_t is a significant change point at level α (Du et al. 2013).

Teleconnection of global atmospheric circulation and drought indices

In this study, Pearson's correlation coefficient (r) was used to examine the link of seasonal and annual drought indices (SPI/SPEI) with tropical SSTs anomalies at the 95%confidence level. It measures the linear association between two variables x_i and y_i. The Pearson correlation (r) is given by

$$r = \frac{\sum_{i=1}^{n}(x_i - \bar{x})(y_i - \bar{y})}{\sqrt{\sum_{i=1}^{n}(x_i - \bar{x})^2 (y_i - \bar{y})^2}} \tag{16}$$

where: n is the number of observations, x, and y the variables and $\bar{x}$ and $\bar{y}$ are their mean, respectively. The relation coefficient (r) takes values between the + 1 and − 1; where: + 1 perfect positive that indicates as the value of one variable increase, there is the predictable variable increase and 0 is no relationship, as well as − 1, indicates that the value of one variable increase the predictable variable is decreased.

The current study was conducted following specific properly arranged methodologies. Therefore, Fig. 3 concise the framework of the methodology.

Results

Trend and changing point of rainfall and temperature

The mean annual rainfall was 1112.73 mm, ranging from 922.82 to 1289.81 mm. The Kiremt (JJAS) season is the primary rainy season, contributing 56.66% of the total rainfall. The Belg (FMAM) is the second rainy season, contributing about 29.25% of the annual rainfall.

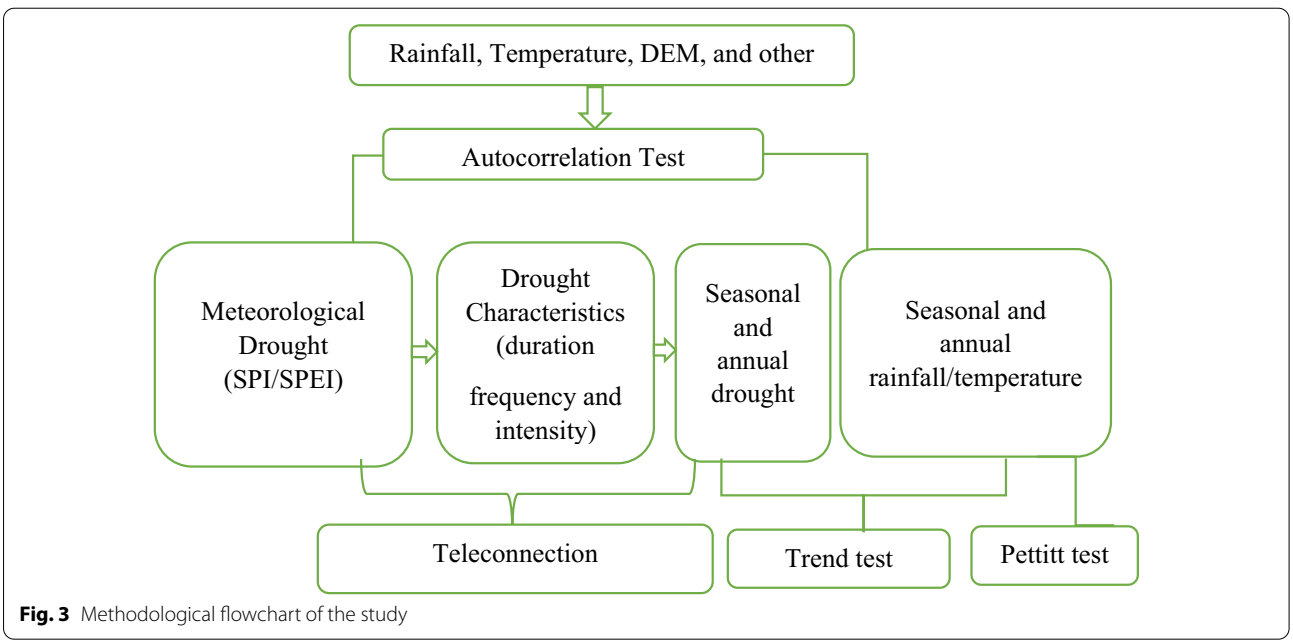

Fig. 3 Methodological flowchart of the study

In evaluating trends, mean seasonal and annual rainfall decreased in the basin. The Belg season rainfall decreased significantly by 2.97 mm/year (Table 3). The Belg rainfall illustrated a significant downward at the change point in 1996. The mean annual temperature was 22.64 °C, the mean minimum and the maximum temperature were 13.35 and 31.14 °C, respectively. The trend test result shows that the mean Belg, Kirmet, Bega season, and annual temperature exhibited a significant increase at change points in the year 1996, 2000, and 1999 (Table 3). The increasing temperature observed in the basin significantly impacts soil water demand and enhances the raising of evapotranspiration that makes more water loss.

The mean temporal evaluation of drought events

Figure 4 shows the temporal distribution of drought occurrence over OGRB. To evaluate the temporal variation, drought events in the basin which are consecutively less than a threshold value (SPI/SPIE ≤ -1) and have more than 4 months duration, have been selected. Hence, in the basin for seasonal drought (SPI-4), moderate, severe, and extreme droughts occurred for 21,

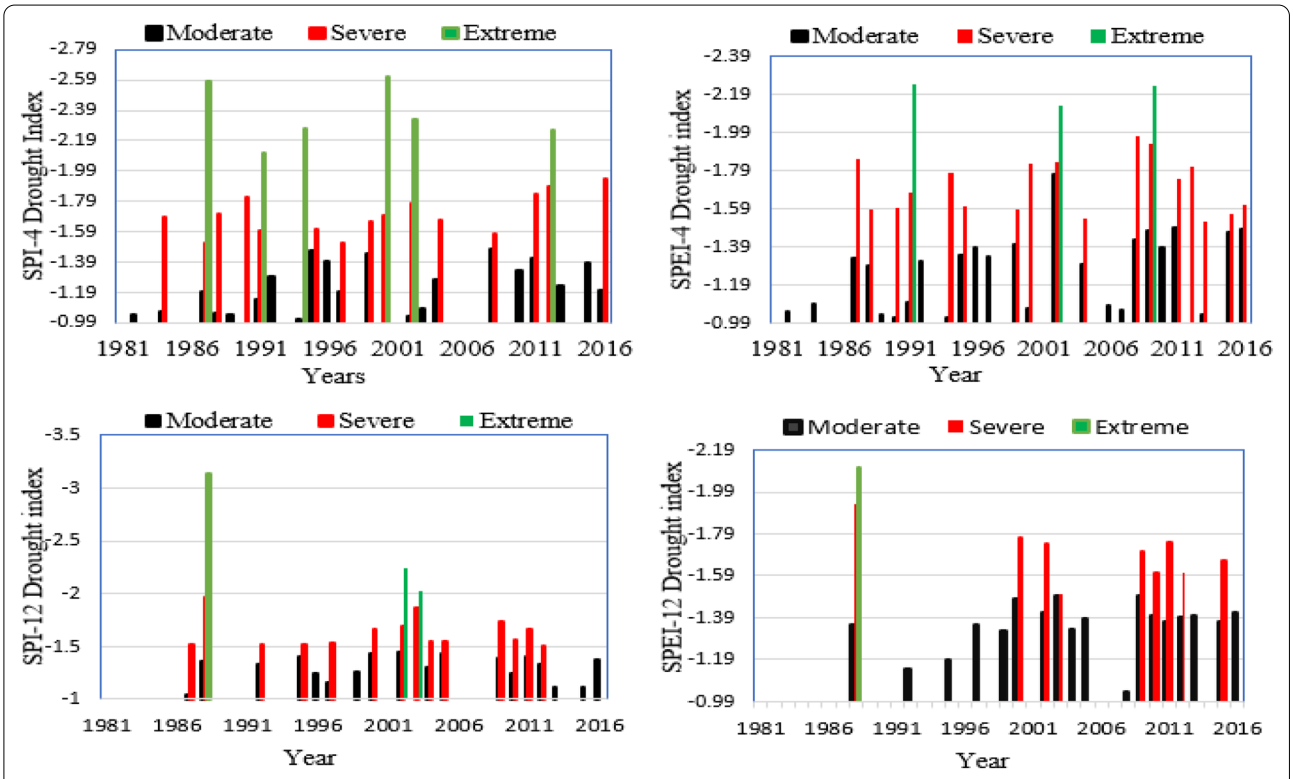

Fig. 4 Evaluation of the mean SPI/SPEI for 4- and 12-month timescales for moderate, severe, and extreme drought events in OGRB from 1981 to 2017

Table 3 Mean seasonal and annual rainfall and temperature trend as well as change point, from 1981 to 2017

Variables	Seasons	Mean value	Sens' slope	Changing point
Rainfall (mm)	Belg(FMAM)	325.625	**−2.971***	**1996***
	Kirmet (JJAS)	630.571	−1.59	1998
	Bega (ONDJ)	156.293	−0.463	1984
	Annua	1112.735	−1.87	1996
Mean temperature T_{mean} (°C)	Belg (FMAM)	21.23	**0.057***	**1996***
	Kiremt (JJAS)	20.12	**0.042***	**1996***
	Bega (ONDJ)	23.29	**0.045***	**2000***
	Annual	22.64	**0.048***	**1999***

* Bold values represent statistically significant at $P < 0.05$, rainfall trend (mm/year), and temperature trend (0C/year)

15, and 6 years, respectively, whereas in 1987, 1991, 1994, 2000, and 2002 extreme droughts occurred. For annual drought (SPI-12), moderate, severe, and extreme droughts were found for 18, 14 and 3 years, respectively whereas in the years 1988, 2002, and 2003 extreme droughts were observed. For seasonal drought (SPEI-4), moderate, severe, and extreme droughts occurred for 25, 17 and 3 years, respectively, while extreme droughts were exhibited in 1991, 2002, and 2009. For annual drought events (SPEI-12), moderate, severe, and extreme droughts were detected for 18, 9, and 1 year, respectively, while in the year 1988, extreme drought was observed.

The number of drought duration months shown in 12-month timescales was 78 and 88 for SPI-12 and SPEI-12, respectively, throughout the study period. In the basin, 1988, 1999, 2000, 2002, 2003, 2012, 2015, and 2016 were the driest years common in both indices and in different timescales. During the study period, the basin experienced 12.6% to 20.36% moderate and above moderate drought frequencies. In SPI-4 and SPEI-4, severe drought events were observed in the basin on March 2000 and July 2009, with the severity peak values of -2.61 and -2.24, respectively. For SPI-12 and SPEI-12, the basin experienced extreme drought in May 1988 (in both indices) with a severity value of -3.13 and -2.10, respectively.

The duration and frequency of drought events distribution

In this study, the duration and frequency of drought occurrence from moderate to extreme drought values were calculated based on the threshold value (SPI/SPEI ≤ -1) in the whole study period. The stations are grouped into three sub-basins to see the distribution of drought duration in the basin. The duration of moderate drought events ranged from 34 to 62 for SPI/SPEI-4 and from 29 to 68 for SPI/SPEI-12. The duration of severe drought events ranged from 12 to 29 for SPI/SPEI-4 and 9 to 47 for SPI/SPEI-12. The duration of extreme drought events ranged from 2 to 20 for SPI/SPEI-4 and from 0 to 18 for SPI/SPEI-12 (Table 4).

The highest drought frequency was observed for different timescales in the southern part and decreased towards the northern and central parts (Fig. 5). The drought frequency was higher for SPEI-4 and SPEI-12 than SPI in both timescales. The higher frequency of drought events was exhibited for SPI-4 and the SPEI-4 almost in all parts of the southern sub-basin.

Table 4 Range of duration (number of months) of moderate, severe, and extreme drought events in the sub-basins

Sub-basin	Drought category	SPI-4	SPEI-4	SPI-12	SPEI-12
Northern	Moderate	37–47	43–55	31–45	42–61
	Severe	14–29	21–25	9–41	9–32
	Extreme	5–15	2–6	6–17	1–9
Central	Moderate	33–54	46–55	29–62	35–59
	Severe	12–23	17–24	9–21	16–26
	Extreme	3–18	2–7	1–16	0–12
Southern	Moderate	34–57	47–62	38–48	38–68
	Severe	16–29	17–29	8–47	19–22
	Extreme	8–20	3–7	5–18	0–14

The temporal and spatial variation of drought characteristics

Tables 5, 6, and 7 show the duration, magnitude, and intensity of occurrence of the significant drought events (SPI/SPEI ≤ -1). According to Eqs. 7, 8, and 9, the duration, magnitude, and intensity of drought events calculated based on SPI/SPEI were consecutively equal or less than the threshold value.

Drought characteristics in the northern part of OGRB

Table 5 shows the drought characteristics observed in the northern parts of OGRB. In this sub-basin, the most extended continuous duration (13-months) of drought event was observed at the Gibe Farm station for SPI-4, while 59 series months of drought duration were observed at the Gedo station SPI-12. Sixteen months of continuous drought events were observed at the Gedo station for SPEI-4. The most prolonged continuous drought duration (69-months) was observed in this sub-basin at the Wolkite station for SPEI-12. During the last 15 years, the droughts were longer and more intense than in the first 15 years in the study period. In the northern part of the basin, the highest magnitude and intensity were observed at Gedo and Ambo stations -84.88 and -1.68, respectively.

Drought characteristics in Central part of OGRB

Table 6 shows the drought characteristics obtained in the central part of OGRB, including stations; Bonga, Jimma, and Shebe. In this sub-basin, the most prolonged duration of drought event for SPI-4 was 14 months, which was shown at the Bonga station, while for SPI-12, 23-months of duration was observed at Yayaotona stations. In the central part, the most extended drought events for SPEI-4 were 20 months observed at Bele station, whereas

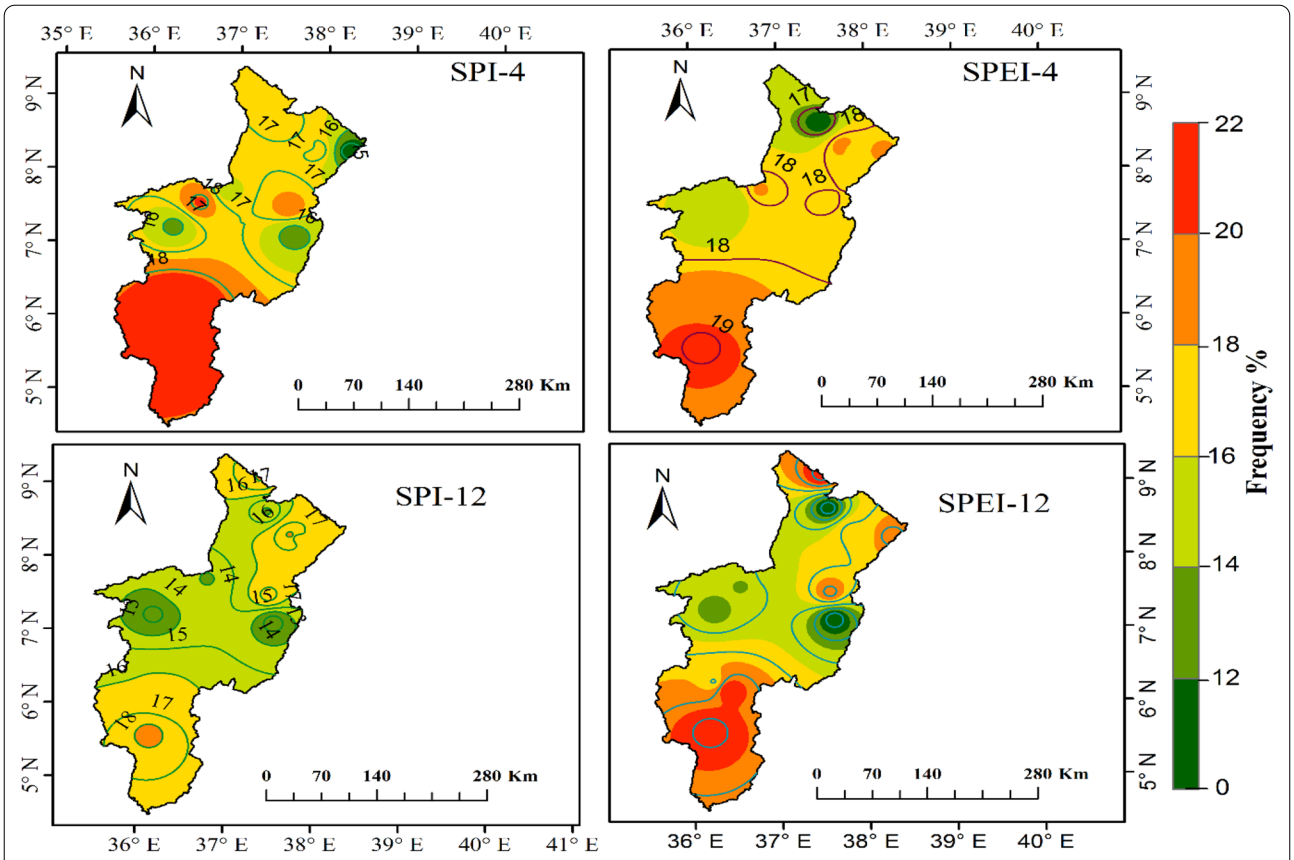

Fig. 5 Spatial distribution of drought frequency in different degrees for SPI/SPEI in 04- and 12-time scale in OGRB from 1981 to 2017

for SPEI-12, the most extended continuous drought duration of 34 months was observed at Bonga station. In this sub-sub basin, the highest magnitude and intensity are shown at Bonga and Shebe stations of −44.4 and −2.24, respectively. The magnitude of drought events in the central part of the basin was less than in the northern and the southern parts of OGRB because the central part is a humid region compared to the other parts of the basin.

Drought characteristics in the southern part of OGRB

Table 7 shows the drought characteristics result obtained in the southern part of OGRB. In this sub-basin, the most extended duration of drought events for SPI-4 was 11 months, observed at Jinka station, whereas for SPI-12 months, 53 months drought duration was observed at Sawla stations. The most extended duration of drought events for SPEI-4 in this sub-basin was 13 months observed at Morka station, whereas 72 months drought duration was observed at Sawla stations for SPEI-12 months. The magnitude and intensity were enormous in these semiarid and arid parts of the basin. In this sub-basin, long and intense drought events were observed from 1999 to 2015. In the southern part of the basin, the highest magnitude and intensity of droughts were shown at Sawla and Jinka stations, respectively (Table 7). Moreover, the highest peak values in this sub-basin ranged from −3.02 to −4.89 were observed.

Seasonal and annual trend analysis of drought events

Figure 6. illustrates the seasonal trend of drought indices in the basin using both Z value and sens slope estimators. The negative value of Z represents a drying tendency and vice versa. All stations depicted a drying trend in the Belg (FMAM) season for SPI-4. Among these stations, Ambo, Bele, Bonga, Gedo, Jimma, Sawla, and Wolkite stations exhibited a significant drying trend. In the Belg season for SPEI-4, all stations showed an increasing drying trend. The Belg season for SPEI-4, including Gibe Farm and the previous seven stations, depicted a significant increase in drought. The slopes of the drying rate at these eight stations were −0.045, −0.42, −0.05, −0.03, −0.05, −0.04, −0.001 and −0.05/year, respectively. All stations showed a drying trend for SPI/SPEI-4 in the Kiremt (JJAS) season except for Gibe Farm and Morka stations. However, these two stations showed an insignificant wetting tendency. In Cermet (JJAS) season, Ambo, Bonga, and Sawla stations

Table 5 The significant drought events (SPI/SPEI ≤ -1) duration, magnitude, intensity, and peak value in the northern part of OGRB from 1981 to 2017

Sub-basin	Stations	Accumulation periods	Duration	Magnitude	Intensity	Peak value
Northern	Ambo	SPI-4	Apr 1991–Dec 1991	−10.4	−1.16	−2.76
		SPI-12	May 2002–Sep 2004	−30.20	−1.68	−2.32
		SPEI-4	Apr1990–Dec1991	−10.18	−1.3	−2.37
		SPEI-12	Jul 2002–Feb 2005	−35.92	−1.12	−2.61
	Butajira	SPI-4	July1997–Jun1988	−17.34	−1.58	−3.39
		SPI-12	Oct 1990–Jun 1992	−30.96	−1.35	−2.83
		SPEI-4	Oct1990–Jan1992	−20.23	−1.26	−2.22
		SPEI-12	Oct 2014–Mar 2017	−21.81	−1.21	−2.43
	Gedo	SPI-4	Nov 2010–Nov 2011	−21.14	−1.42	−2.72
		SPI-12	Sep 1995–Jul 2000	−84.88	−1.44	−2.36
		SPEI-4	Nov 1998–Dec 1999	−19.86	−1.42	−2.11
		SPEI-12	May 2011–Jun 2012	−22.2	−1.59	−1.84
	Gibe Farm	SPI-4	Dec 1999–Dec 2000	−17.6	−1.35	−2.98
		SPI-12	Jul 2002–Feb 2005	−45.53	−1.42	−3.41
		SPEI-4	Dec1999–Dec 2000	−16.05	−1.23	−2.17
		SPEI-12	Jul 2000–Apr 2005	−40.31	−1.19	−2.23
	Wolkite	SPI-4	Feb 2000–Nov 2000	−13.25	−1.2	−3.38
		SPI-12	Sep 1999–May 2001	−31.93	−1.52	−2.74
		SPEI-4	Mar 1999–Dec 2000	−13.25	−1.2	−3.58
		SPEI-12	Sep 1999–May 2005	−76.24	−1.10	−1.95

Table 6 The significant drought events (SPI/SPEI ≤ -1) duration, magnitude, intensity, and peak value at the central part of OGRB from 1981 to 2017

Sub-basin	Stations	Accumulation periods	Duration	Magnitude	Intensity	Peak value
Central	Bele	SPI-4	May 1990–Feb 1991	−13.35	−1.34	−2.39
		SPI-12	Jul 2002–Jul 2003	−23.89	−1.84	−2.27
		SPEI-4	Jun1990–Jan1992	−21.39	−1.1	−2.16
		SPEI-12	Jul 1990–Dec 1991	−25.81	−1.36	−2.32
	Bonga	SPI-4	Aug 1996–Sep 1997	−30.99	−2.20	−3.61
		SPI-12	Oct 1994–Dec 1995	−20.20	−1.35	−3.37
		SPEI-4	Aug 1996–Aug 1997	−21.59	−1.66	−2.28
		SPEI-12	Dec 2010–Sep 2013	−44.32	−1.30	−2.36
	Jimma	SPI-4	Aug 2003–Aug 2004	−14.27	−1.1	−3.37
		SPI-12	Jun 2011–Apr 2013	−27.28	−1.19	−2.41
		SPEI-4	Aug 2003–Sep 2004	−17.36	−1.24	−2.29
		SPEI-12	Jun 2011–Dec 2013	−34.16	−1.10	−2.27
	Shebe	SPI-4	Feb 2002–Dec 2002	−24.35	−2.20	−3.62
		SPI-12	Apr1994–Dec 1995	−29.38	−1.40	−3.74
		SPEI-4	Oct 1994–Oct 1995	−20.80	−1.39	−2.29
		SPEI-12	Jan 1994–Apr 1996	−45.40	−2.24	−2.11
	Yayaotona	SPI-4	Feb 2000–Sep 2000	−10.89	−1.36	−2.85
		SPI-12	Apr 1999–Feb 2001	−31.75	−1.38	−2.19
		SPEI-4	Feb 2000–Sep 2000	−10.69	−1.33	−2.23
		SPEI-12	Apr 1999–Feb 2001	−33.64	−1.46	−1.97

Table 7 The significant drought events (SPI/SPEI ≤ − 1) duration, magnitude, intensity, and peak value in the south part of OGRB from 1981 to 2017

Sub-basin	Stations	Accumulation periods	Duration	Magnitude	Intensity	Peak value
Southern	Jinka	SPI-4	Nov 1996–Sep 1997	− 24.3	− 2.27	− 4.89
		SPI-12	Jun 1999–Sep 2000	− 32.78	− 2.05	− 3.22
		SPEI-4	Sep 1993–Apr 1994	− 12.18	− 1.52	− 2.25
		SPEI-12	Jun 1999–Dec 2000	− 39.94	− 2.10	− 2.36
	Morka	SPI-4	Mar 2009–Sep 2009	− 13.37	− 1.91	− 3.02
		SPI-12	Aug 2011–Mar 2012	− 25.93	− 2.16	− 2.25
		SPEI-4	Apr 1999–Apr 2000	− 17.65	− 1.36	− 2.32
		SPEI-12	Mar 1988–Apr 1991	− 59.54	− 1.57	− 2.16
	Sawla	SPI-4	Oct 2010–Jun 2012	− 29.51	− 1.41	− 3.54
		SPI-12	May 2007–Feb 2010	− 80.85	− 1.53	− 2.76
		SPEI-4	Oct 2010–Jun 2012	− 31.02	− 1.48	− 2.38
		SPEI-12	Apr 2011–Jan 2017	− 86.83	− 1.21	− 1.98

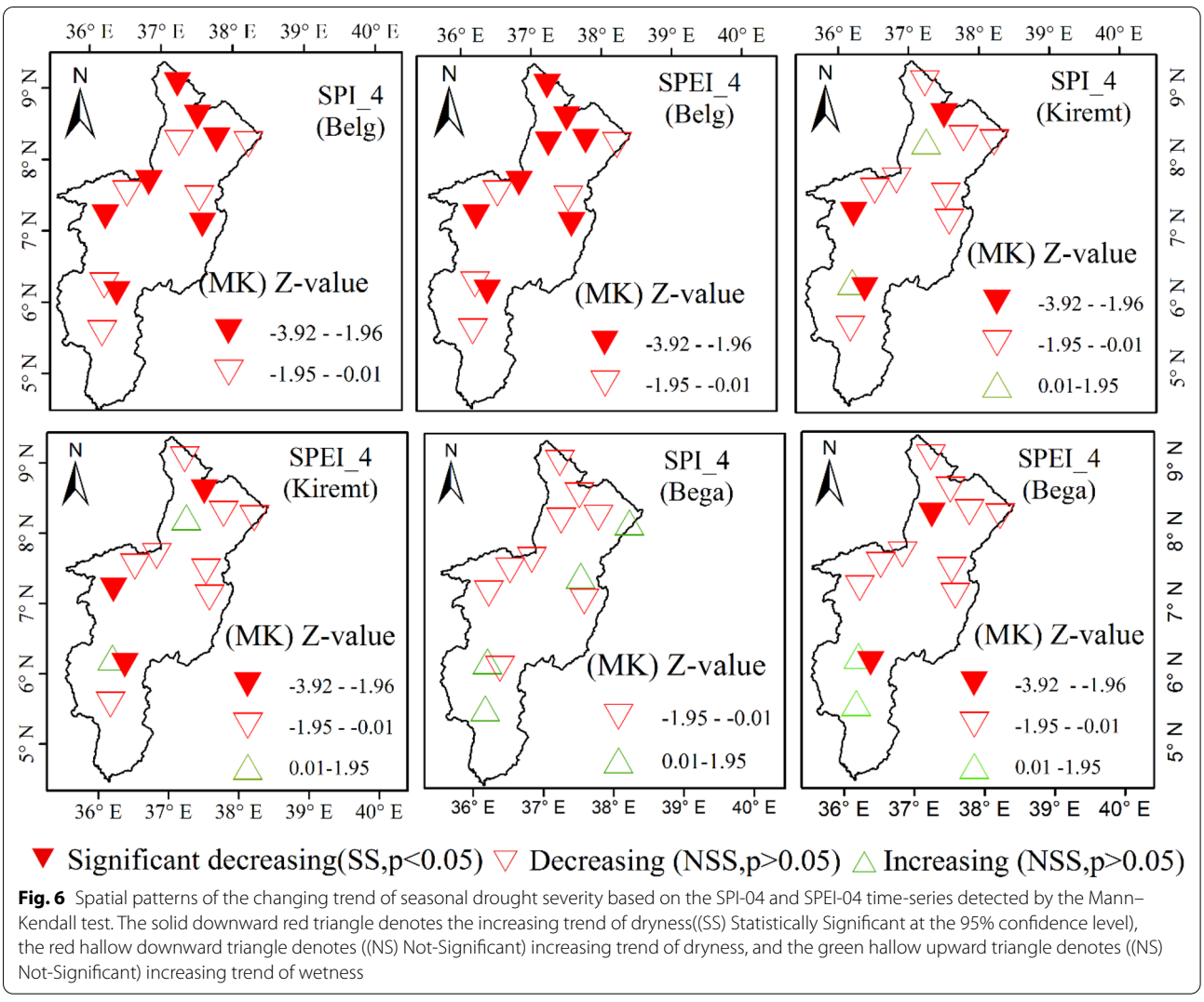

Fig. 6 Spatial patterns of the changing trend of seasonal drought severity based on the SPI-04 and SPEI-04 time-series detected by the Mann–Kendall test. The solid downward red triangle denotes the increasing trend of dryness((SS) Statistically Significant at the 95% confidence level), the red hallow downward triangle denotes ((NS) Not-Significant) increasing trend of dryness, and the green hallow upward triangle denotes ((NS) Not-Significant) increasing trend of wetness

depicted a significant increasing drought trend for SPI-4 and SPEI-4.

The Bega (ONDJ) is the second rainy season for the southern part of OGRB. For SPI-4 of Bega season, Butajira, Jinka, Morka, and Yayaotona stations illustrated decreasing drying events. In comparison, the rest of 70% of stations in the basin showed a drying tendency. In the Bega season (SPEI-4), except Jinka and Sawla station, 84% of the stations showed an increasing trend of drought events. However, a significant increase in drought was observed in Gibe Farm and Sawla station for SPEI-4.

Figure 7 shows the annual drought trend test in the basin. Accordingly, in the annual drought trend evaluation for the SPI-12, a significant increasing trend was observed at Ambo and Sawla stations. For SPEI-12, a significant increase in drought tendency was observed in Ambo, Bonga, Jimma, Sawla, and Wolkite stations. The result of the trend analysis for SPI/SPEI-12 depicts the increase of drought events in the entire basin. This annual drought affects almost all the determinants of the hydrological cycle in the area.

Teleconnection of drought indices with global climate variability

The base of all types of droughts originates from the deficiency in precipitation that is derived by global sea surface temperature (Ionita et al. 2012). This study investigated the association of global climate anomalies on the frequency of drought events in the basin (Fig. 8). The Belg and Kirmet seasonal indices (SPI04/SPEI04) were taken to represent the two main rainy seasons in the basin. Accordingly, Fig. 8 shows a negative link between Nino3.4 and seasonal drought indices. The higher correlations ($r = -0.43$ to -0.51) of NINO3.4 with Belg and kirmet season drought incidences were exhibited. The result indicates that NINO3.4 intensifies the seasonal

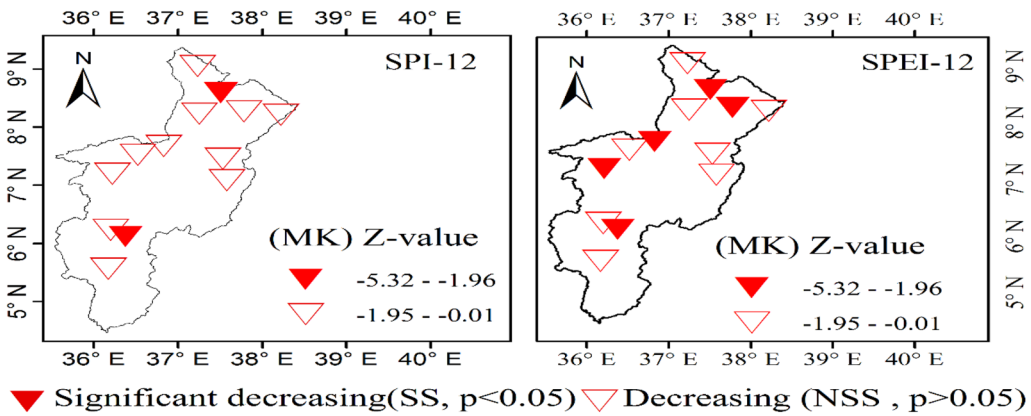

Fig. 7 Spatial patterns of the changing trend of seasonal drought severity based on the SPI-12 and SPEI-12 time-series detected by the Mann–Kendall trend test. The solid downward red triangle denotes the increasing dryness trend Statistically Significant (SS) at the 95% confidence level. The red hallow downward triangle denotes Not-Significant (NS) increasing dryness

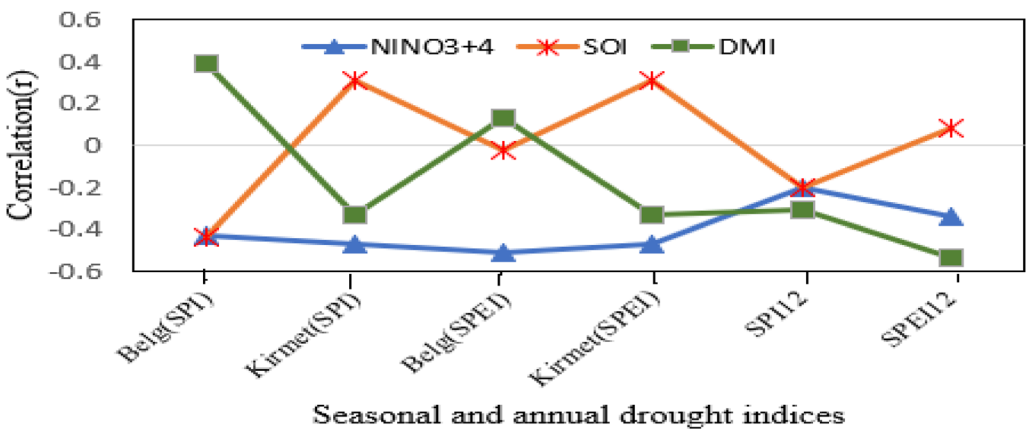

Fig. 8 Teleconnections of seasonal and annual drought indices (SPI/SPE) with global climate indices

drought in the basin. The NINO3.4 also has a considerable negative correlation with annual drought SPEI12. The SOI has a pronounced positive/negative correlation with seasonal and annual drought indices. Mainly, SOI observed a significant negative correlation ($r = -0.44$) with Belg (SPI04) season drought occurrence in the basin. The association between SOI and the Kirmet (SPI04/SPEI04) was positive, indicating its influence on drought reduction in the area. The teleconnection between seasonal and annual drought incidences with DOI was positive/negative (Fig. 7). The DOI was supplied Belg season rainfall and significantly influenced the intensification of annual drought (SPEI12). Mainly, the NINO3.4 and SOI intensify the Belg season drought occurrence in the area. The NINO3.4 and DOI have a significant negative correlation ($r = -0.4$ and -0.53) with annual drought indices (SPEI12) that depicted the influence of the two indices on the intensification of annual drought occurrence (Fig. 8).

Discussion

In this study, the analysis of meteorological data evaluation depicts the variability of rainfall and temperature trend during the study period. The trend test of rainfall shows high variability and the insignificant decreasing trend of mean annual and seasonal rainfall except for the Belg season in the basin. A significant change point of mean Belg rainfall was observed in 1996. On the other hand, the mean annual and seasonal temperature increased significantly in the basin during the study period. The significant changing point of mean Belg, Kirmet, Bega season, and annual temperature exhibited in 1996, 1996, 2000, and 1999, respectively. This finding is in agreement with Funk et al. (2005), Getachew Alem (2018), who reported an increase in temperature and decreasing rainfall trend in Ethiopia's southern and southwestern regions. In line with these findings, Esayas et al. (2018) also reported that the trend of warm extremes was increasing in southwestern Ethiopia, which implies the significant warming of the area. Thus, these meteorological extremes intensify hydrological hazards (drought) and cause several destructions in different sectors.

According to the studies done by Meza (2013), the SPEI is crucial for recognizing the role of temperature or global warming on drought conditions better than SPI. Therefore, in addition to the SPI, the SPEI indices were used to analyze the drought characteristics in the basin. The temporal and spatial increase of drought was observed predominantly from 1999 to 2016. The most prolonged duration of drought events is shown in 2000, 2002, and 2003. For SPEI-12, the most prolonged severe duration of drought events was exhibited from 2000 to 2016.

The distribution of drought characteristics found in the basin was complex and had noticeable spatial and temporal variations. The overall result indicates that the prolonged drought duration and severe intensities of drought events were recorded in the southern parts and decreased towards the northern parts of the basin. However, a considerable amount of the drought frequency and drought magnitude and intensity have been observed in the central and northern part of the basin, which previously had no record of drought incidences. This occurrence of drought incidences in the upper streams (northern and central parts) affects the agricultural and hydropower production as well as irrigation activities done in the downstream or low lands (pastoral area) of OGRB (Amsalu and Adem 2009). Notably, this lowland part of the basin receives very less annual rainfall. Similarly, FAO (2017) pointed out that the drought of 2011 and 2016 devastated Ethiopia's pastoral and agropastoral livelihoods.

The seasonal drought trend analysis depicted a significant increase in the seasonal drought risk in most basin parts, mainly in the Belg (FMAM) season. This result was considered problematic because the Belg season is typically wet season for the two rainfall regimes. In addition, the basin's southern part relies strongly on the Belg season rainfall (Viste et al. 2013). In this season, a significant increasing trend of drought frequency was observed at more than 53% of stations in the basin. The seasonal trend analysis of drought depicts an increasing trend of drought events in the Kiremt (JJAS) season almost in all stations except at Gibe Farm and Morka stations. During the Bega (ONDJ) season, a significant increasing trend of drought frequency is observed in the southern sub-basin. Even if the Bega season is the driest season for the central and northern parts of the basin, the smallest amount of rain obtained in the Bega is very important for preparing farming land with limited soil moisture. Nevertheless, the drought occurrence in the Bega season has impacted the agricultural and mainly pastoral activities in the low land parts of the basin.

These increasing seasonal drought trends in the OGRB agreed with the study done by Seleshi and Camberlin (2006), who found that the decline of seasonal rainfall caused food shortages in the area. However, the results of this study contradict the previous study of Degefu and Bewket (2014) that reported the reviving of rainfall in the basin during the last two decades. The annual drought trend test for SPI-12 and SPEI-12 showed the increasing trend of drought events in all basin parts. The increasing trend of the annual drought was more significant in SPEI than SPI. It is also possible in the case of the region's significantly increased temperature and evapotranspiration. The increasing drought incidences in several parts of the

world are mainly linked to the lack of precipitation, air temperature rise, and atmospheric evapotranspiration demand (Mohammed et al. 2020). Therefore, this increment of annual drought incidence causes water stress for the basin's hydropower production and irrigation activities.

The teleconnection analysis results depict the seasonal and annual drought in the basin driven by global climate indices. The variability of Belg and Kirmet season droughts in the OGRB was highly correlated with global climate indices such as NINO3.4 and SOI. Remarkably, the seasonal intensification of drought in this study area was triggered by the NINO3.4 and SOI. This finding is concise with Tesfamariam et al. (2019), Woldegebrael et al. (2020), who reported that the frequent extreme incidence in the spring and summer seasons could be mainly linked in Ethiopia Nino3.4 anomalies. Getachew Alem (2018) also reported that the recent El Niño-induced drought of 2015/2016 has led to severe impact in lowland pastoralist areas of the country, including this basin.

The most important finding that the current study highlights are the intensification of severe and extreme drought events, including the wettest regions found in the northern and central parts of OGRB. The study identified global signals that influenced the drought intensification in the area. Remarkably, the drought occurrence in northern and central parts has a significant adverse effect on the water availability downstream, where massive hydropower and irrigation dams are found. Overall, increasing the frequency and intensity of agricultural and annual drought events in the entire basin is an alarming event to think over. Therefore, this finding may allow for better planning of the efficient use of water resources and hydropower and agricultural production in the entire basin.

Conclusion

This study evaluated the spatiotemporal characteristics and trends of drought in OGRB using SPI and SPEI in 4- and 12-months timescales from 1981 to 2017. It examined the drought characteristics in this particular basin in terms of duration, frequency, intensity, and spatial extent. This study applied Ethiopia's four months seasonal division (Belg, Kirmet, and Beg), which depicts the country's regional rainfall patterns. Hence the results would be helpful to the local scale applicability of drought indices. Compared to SPI, SPEI captured a higher number of moderate and severe drought events. Erratic rainfall, consistent rising temperature, and increasing potential evapotranspiration made the basin experience severe drought conditions. A statistically significant increase in severe and extreme drought events in the basin was observed over the last seventeen years (1999–2016). The distribution of drought characteristics has high spatial and temporal variation. Even the wettest parts of the basin (the northern and central parts) also experienced severe drought events during the study period. This spatiotemporal characteristic and trend analysis of drought provide better insight into the higher frequency, intensity, and increasing drought tendency in OGRB. Apart from other local factors, the study found that Niño3.4, SOI, and DMI have a functional influence on drought occurrence in the area. The strongest negative correlations were observed between Niño3.4 and seasonal drought (Belg and Kirmet) that influenced the intensification of drought in the area. Therefore, the result of the study provides valuable information on regional drought frequency, severity, intensity, trend, and the global driver's influence on drought occurrence in the OGRB. The study plays a significant role in developing drought mitigation plans and water resource management systems.

Limitations of the methodology and the need for future research

A lack of literature on drought in the area makes comparative analysis more challenging. To apply more drought indices in the study is difficult because the only data obtained from NMA were rainfall and temperature, and it is impossible to get other data such as the streamflow and other climate variables. Therefore, future drought analysis in the basin must consider other indices to elaborate the basin's drought characteristics in terms of other hydroclimate variables.

Acknowledgements

The authors greatly appreciate the National Meteorology Agency of Ethiopia for providing meteorological data.

Authors' contributions

FAA: conceptualization; data curation; formal analysis, investigation writing-original draft preparation. KTB: supervision, reviewing and editing, visualization, investigation, funding acquisition. TTZ: software, writing-reviewing and editing and validation. GLF: reviewing and editing, supervision, validation. DYA: reviewed and edited the language. BTH: reviewing and editing, supervision, validation. All authors read and approved the final manuscript.

Funding

This study partially got funded by Addis Ababa University for data collection and processing only.

Availability of data and materials

The data used to have the findings of this study are submitted as an additional file.

Declarations

Ethics approval and consent to participate

This research paper is part of the thesis 'Historical trend analysis and model projection of climate change impacts on the hydrological cycle in the case of Omo-Gibe River Basin, Ethiopia.' Therefore, all authors approve to publish the findings, and there is no ethical conflict.

Consent for publication
All authors read the manuscript and agreed to publication.

Competing interests
The authors declare that they have no competing interests.

Author details
[1]Center for Environmental Science, College of Natural and Computational Sciences, Addis Ababa University, P. O. Box 1176, Addis Ababa, Ethiopia. [2]Institute of Geophysics Space Science and Astronomy, Addis Ababa University, PO Box 1176, Addis Ababa, Ethiopia. [3]Center for Food Security Studies, College of Development Studies, Addis Ababa University Ethiopia, Addis Ababa University, PO Box 150129, Addis Ababa, Ethiopia.

Received: 8 October 2021 Accepted: 14 February 2022
Published: 15 March 2022

References

Alamgir M, Shahid S, Hazarika MK et al (2015) Analysis of meteorological drought pattern during different climatic and cropping seasons in Bangladesh. J Am Water Resour Assoc 51:794–806. https://doi.org/10.1111/jawr.12276
Alexander LV, Tapper N, Zhang X et al (2009) Climate extremes: progress and future directions. Int J Climatol 29:317–319. https://doi.org/10.1002/joc.1861
Allen RG, Pereira LS, Raes D, Smith M (1998) Crop evapotranspiration-Guidelines for computing crop water requirements-FAO Irrigation and drainage paper 56. Fao, Rome 300:D05109
Alsafadi K, Mohammed SA, Ayugi B et al (2020) Spatial-temporal evolution of drought characteristics over hungary between 1961 and 2010. Pure Appl Geophys 177:3961–3978. https://doi.org/10.1007/s00024-020-02449-5
Amsalu A, Adem A (2009) Assessment of climate change-induced hazards, impacts and responses in the southern lowlands of Ethiopia. In: Forum for Social Studies (No. 4). Forum for Social Studies (FSS)
Andreadis KM, Clark EA, Wood AW et al (2005) Twentieth-century drought in the conterminous United States. J Hydrometeorol 6:985–1001. https://doi.org/10.1175/JHM450.1
Asong ZE, Wheater HS, Bonsal B et al (2018) Historical drought patterns over Canada and their teleconnections with large-scale climate signals. Hydrol Earth Syst Sci 22:3105–3124. https://doi.org/10.5194/hess-22-3105-2018
Avery S (2010) Hydrological impacts of Ethiopia's Omo basin on Kenya's Lake Turkana water levels and fisheries. Final report prepared for the African Development Bank, Tunis.
Beguería S, Vicente-Serrano SM, Angulo-Martínez M (2010) A multiscalar global drought dataset: the SPEIbase: a new gridded product for the analysis of drought variability and impacts. Bull Am Meteorol Soc 91:1351–1354
Beguería S, Vicente-Serrano SM, Reig F, Latorre B (2014) Standardized precipitation evapotranspiration index (SPEI) revisited: parameter fitting, evapotranspiration models, tools, datasets and drought monitoring. Int J Climatol 34:3001–3023. https://doi.org/10.1002/joc.3887
Changnon SA (2000) El Niño 1997–1998: the climate event of the century. Oxford University Press
Degefu MA, Bewket W (2015) Trends and spatial patterns of drought incidence in the omo-ghibe river basin, ethiopia. Geogr Ann Ser A Phys Geogr 97:395–414. https://doi.org/10.1111/geoa.12080
Degefu MA, Bewket W (2014) Variability and trends in rainfall amount and extreme event indices in the Omo-Ghibe River Basin, Ethiopia. Reg Environ Chang 14:799–810. https://doi.org/10.1007/s10113-013-0538-z
Degefu MA, Rowell DP, Bewket W (2017) Teleconnections between Ethiopian rainfall variability and global SSTs: observations and methods for model evaluation. Meteorol Atmos Phys 129:173–186. https://doi.org/10.1007/s00703-016-0466-9
Degefu W (1987) Some aspects of meteorological drought in Ethiopia. In: Glantz MH (ed) Drought and Hunger in AfricaWorkineh. Cambridge University Press, Cambridge
Dinku T, Funk C, Peterson P et al (2018) Validation of the CHIRPS satellite rainfall estimates over eastern Africa. Q J R Meteorol Soc 144:292–312. https://doi.org/10.1002/qj.3244
Dinku T, Hailemariam K, Maidment R et al (2014) Combined use of satellite estimates and rain gauge observations to generate high-quality historical rainfall time series over Ethiopia. Int J Climatol 34:2489–2504. https://doi.org/10.1002/joc.3855
Du J, Fang J, Xu W, Shi P (2013) Analysis of dry/wet conditions using the standardized precipitation index and its potential usefulness for drought/flood monitoring in Hunan Province, China. Stoch Environ Res Risk Assess 27:377–387. https://doi.org/10.1007/s00477-012-0589-6
Dubache G, Ogwang BA, Ongoma V, Islam ARMT (2019) The effect of Indian Ocean on Ethiopian seasonal rainfall. Meteorol Atmos Phys 131:1753–1761
EEPC (Ethiopian Electric power Corporation) (2010) Gibe III hydroelectric project: environment & social issues related to Gibe III hydroelectric,Gibe III HEP Office, Addis Ababa, Ethiopia
Endris HS, Lennard C, Hewitson B et al (2016) Teleconnection responses in multi-GCM driven CORDEX RCMs over Eastern Africa. Clim Dyn 46:2821–2846
Esayas B, Simane B, Teferi E, et al (2018) Trends in extreme climate events over three agroecological zones of southern Ethiopia. Adv Meteorol 2018:
Fanta D, Disse M (2018) Analyzing the future climate change of Upper Blue Nile River basin using statistical downscaling techniques. Hydrol Earth Syst Sci 22:2391–2408. https://doi.org/10.5194/hess-22-2391-2018
FAO (2017) Ethiopia Drought response plan and priorities. Accessed 08 June 2020
Fenta AA, Yasuda H, Shimizu K, Haregeweyn N (2017) Response of streamflow to climate variability and changes in human activities in the semiarid highlands of northern Ethiopia. Reg Environ Chang 17:1229–1240
Funk C, Senay G, Asfaw A, et al (2005) Recent drought tendencies in Ethiopia and equatorial-subtropical eastern Africa: Washington, DC. FEWS-NET 1:
Funk CC (2012) Exceptional warming in the western Pacific-Indian Ocean warm pool has contributed to more frequent droughts in eastern Africa. Bull Am Meteorol Soc 93:1049–1051
Gebre Michael Y, Hadgu K, Ambaye Z (2005) Addressing pastoralist conflict in Ethiopia: The case of the Kuraz and Hamer sub-districts of South Omo zone,. In: A report submitted to African Peace Forum, EPaRDA, Inter Africa Group, and Saferworld
Gebrechorkos SH, Hülsmann S, Bernhofer C (2019) Changes in temperature and precipitation extremes in Ethiopia, Kenya, and Tanzania. Int J Climatol 39:18–30
Gebrehiwot T, Van der Veen A, Maathuis B (2011) Spatial and temporal assessment of drought in the Northern highlands of Ethiopia. Int J Appl Earth Obs Geoinf 13:309–321
Getachew Alem M (2018) Drought and its impacts in Ethiopia. Weather Clim Extrem 22:24–35. https://doi.org/10.1016/j.wace.2018.10.002
Ghosh KG (2019) Spatial and temporal appraisal of drought jeopardy over the Gangetic West Bengal, eastern India. Geoenvironmental Disasters 6:1. https://doi.org/10.1186/s40677-018-0117-1
Gissila T, Black E, Grimes DIF, Slingo JM (2004) Seasonal forecasting of the Ethiopian summer rains. Int J Climatol A J R Meteorol Soc 24:1345–1358
Giuseppe E, Pasqui M, Magno R, Quaresima S (2019) A counting process approach for trend assessment of drought condition. Hydrology 6:84
Hänsel S, Ustrnul Z, Łupikasza E, Skalak P (2019) Assessing seasonal drought variations and trends over Central Europe. Adv Water Resour 127:53–75
Hargreaves GH, Samani ZA (1985) Reference crop evapotranspiration from temperature. Appl Eng Agric 1:96–99
Ionita M, Lohmann G, Rimbu N et al (2012) Interannual to decadal summer drought variability over Europe and its relationship to global sea surface temperature. Clim Dyn 38:363–377
Irannezhad M, Torabi Haghighi A, Chen D, Kløve B (2015) Variability in dryness and wetness in central Finland and the role of teleconnection patterns. Theor Appl Climatol 122:471–486. https://doi.org/10.1007/s00704-014-1305-x
Jaiswal RK, Lohani AK, Tiwari HL (2015) Statistical analysis for change detection and trend assessment in climatological parameters. Environ Process 2:729–749
Jury MR, Funk C (2013) Climatic trends over Ethiopia: regional signals and drivers. Int J Climatol 33:1924–1935. https://doi.org/10.1002/joc.3560
Kendall MG (1975) Rank Correlation Methods, 4th edn. Griffin. Ltd., London
Khadr M (2016) Forecasting of meteorological drought using Hidden Markov Model (case study: The upper Blue Nile river basin, Ethiopia). Ain Shams Eng J 7:47–56. https://doi.org/10.1016/j.asej.2015.11.005

Kundzewicz ZW, DÖLL P (2009) Will groundwater ease freshwater stress under climate change? Hydrol Sci J 54:665–675. https://doi.org/10.1623/hysj.54.4.665
Labudová L, Labuda M, Takáč J (2017) Comparison of SPI and SPEI applicability for drought impact assessment on crop production in the Danubian Lowland and the East Slovakian Lowland. Theor Appl Climatol 128:491–506
Lautze S, Aklilu Y, Raven-Roberts A, et al (2003) Risk and vulnerability in Ethiopia: Learning from the past, responding to the present, preparing for the future. Rep US Agency Int Dev Addis Ababa, Ethiopia
Liu Z, Wang Y, Shao M et al (2016) Spatiotemporal analysis of multiscalar drought characteristics across the Loess Plateau of China. J Hydrol 534:281–299
Manatsa D, Mushore T, Lenouo A (2017) Improved predictability of droughts over southern Africa using the standardized precipitation evapotranspiration index and ENSO. Theor Appl Climatol 127:259–274
Mann HB (1945) Nonparametric Tests Against Trend. Econom Soc 13:245–259
McKee TB, Doesken NJ, Kleist J (1993) The relationship of drought frequency and duration to time scales. In: Proceedings of the 8th Conference on Applied Climatology. Boston, pp 179–183
Meza FJ (2013) Recent trends and ENSO influence on droughts in Northern Chile: An application of the Standardized Precipitation Evapotranspiration Index. Weather Clim Extrem 1:51–58
Mohammed S, Alsafadi K, Al-Awadhi T et al (2020) Space and time variability of meteorological drought in Syria. Acta Geophys 68:1877–1898
Morid S, Smakhtin V, Moghaddasi M (2006) Comparison of seven meteorological indices for drought monitoring in Iran. Int J Climatol A J R Meteorol Soc 26:971–985
Ntale HK, Gan TY (2003) Drought indices and their application to East Africa. Int J Climatol 23:1335–1357. https://doi.org/10.1002/joc.931
Pal AB, Khare D, Mishra PK, Singh L (2017) Trend analysis of rainfall, temperature and runoff data: a case study of Rangoon watershed in Nepal. Int J Stud Res Technol Manag 5:21–38
Palmer WC (1965) Meteorological drought. US Department of Commerce, Weather Bureau
Pettitt AN (1979) A non-parametric approach to the change-point problem. J R Stat Soc Ser C Applied Stat 28:126–135
Potop V, Možný M (2011) The application a new drought index–Standardized precipitation evapotranspiration index in the Czech Republic. Mikroklima a Mezoklima Kraj Struct a Antropog Prostředí 2:2–14
Richman MB, Leslie LM, Segele ZT (2016) Classifying drought in Ethiopia using machine learning. Procedia Comput Sci 95:229–236
Saji NH, Goswami BN, Vinayachandran PN, Yamagata T (1999) A dipole mode in the tropical Indian Ocean. Nature 401:360–363
Seleshi Y, Camberlin P (2006) Recent changes in dry spell and extreme rainfall events in Ethiopia. Theor Appl Climatol 83:181–191
Sen PK (1968) Estimates of the Regression Coefficient Based on Kendall's Tau. J Am Stat Assoc 63:1379–1389. https://doi.org/10.1080/01621459.1968.10480934
Senay GB, Leake S, Nagler PL et al (2011) Estimating basin scale evapotranspiration (ET) by water balance and remote sensing methods. Hydrol Process 25:4037–4049. https://doi.org/10.1002/hyp.8379
Sharafati A, Nabaei S, Shahid S (2020) Spatial assessment of meteorological drought features over different climate regions in Iran. Int J Climatol 40:1864–1884. https://doi.org/10.1002/joc.6307
Shiferaw H, Gebremedhin A, Gebretsadkan T, Zenebe A (2018) Modelling hydrological response under climate change scenarios using SWAT model: the case of Ilala watershed, Northern Ethiopia. Model Earth Syst Environ 4:437–449. https://doi.org/10.1007/s40808-018-0439-8
Spinoni J, Naumann G, Carrao H et al (2014) World drought frequency, duration, and severity for 1951–2010. Int J Climatol 34:2792–2804
Temam D, Uddameri V, Mohammadi G et al (2019) Long-Term Drought Trends in Ethiopia with Implications for Dryland Agriculture. Water 11:2571. https://doi.org/10.3390/w11122571
Tesfamariam BG, Melgani F, Gessesse B (2019) Rainfall retrieval and drought monitoring skill of satellite rainfall estimates in the Ethiopian Rift Valley Lakes Basin. J Appl Remote Sens 13:14522
Teshome A, Zhang J (2019) Increase of Extreme Drought over Ethiopia under Climate Warming. Adv Meteorol 2019:1–18. https://doi.org/10.1155/2019/5235429
Tian L, Quiring SM (2019) Spatial and temporal patterns of drought in Oklahoma (1901–2014). Int J Climatol 39:3365–3378. https://doi.org/10.1002/joc.6026
Van Loon AF (2015) Hydrological drought explained. Wiley Interdiscip Rev Water 2:359–392. https://doi.org/10.1002/wat2.1085
Vicente-Serrano SM, Beguería S, López-Moreno JI (2010) A Multiscalar Drought Index Sensitive to Global Warming: The Standardized Precipitation Evapotranspiration Index. J Clim 23:1696–1718. https://doi.org/10.1175/2009JCLI2909.1
Viste E, Korecha D, Sorteberg A (2013) Recent drought and precipitation tendencies in Ethiopia. Theor Appl Climatol 112:535–551. https://doi.org/10.1007/s00704-012-0746-3
Wang Q, Wu J, Lei T et al (2014) Temporal-spatial characteristics of severe drought events and their impact on agriculture on a global scale. Quat Int 349:10–21. https://doi.org/10.1016/j.quaint.2014.06.021
Williams AP, Funk C, Michaelsen J et al (2012) Recent summer precipitation trends in the Greater Horn of Africa and the emerging role of Indian Ocean sea surface temperature. Clim Dyn 39:2307–2328. https://doi.org/10.1007/s00382-011-1222-y
WMO (2012) Standardized precipitation index user guide. World Meteorol Organ.
Woldegebrael SM, Kidanewold BB, Zaitchik B, Melesse AM (2020) Rainfall and Flood Event Interrelationship-A Case Study of Awash and Omo-Gibe Basins. Ethiopia. Int J Sci Eng Res 11:80
Workie TG, Debella HJ (2018) Climate change and its effects on vegetation phenology across ecoregions of Ethiopia. Glob Ecol Conserv 13:e00366
Yang C, Tuo Y, Ma J, Zhang D (2019) Spatial and temporal evolution characteristics of drought in Yunnan Province from 1969 to 2018 based on SPI/SPEI. Water Air Soil Pollut 230:269. https://doi.org/10.1007/s11270-019-4287-6
Yue S, Wang CY (2002) Regional streamflow trend detection with consideration of both temporal and spatial correlation. Int J Climatol 22:933–946. https://doi.org/10.1002/joc.781
Zeleke TT, Giorgi F, Diro GT, Zaitchik BF (2017) Trend and periodicity of drought over Ethiopia. Int J Climatol 37:4733–4748. https://doi.org/10.1002/joc.5122

Publisher's Note